

Realization of Li⁺ Domain Diffusion Effect via Constructing of Molecular Brushes on LLZTO Surface and Its Application in All-solid-state Lithium Batteries

Wenwen Li, ^{a,b} Changzhi Sun, ^{a,b} Jun Jin, ^a Yanpei Li, ^{a,b} Chunhua Chen, ^c Zhaoyin Wena, ^{b,*}

a. CAS Key Laboratory of Materials for Energy Conversion, Shanghai Institute of Ceramics, Chinese Academy of Sciences, Shanghai 200050, P. R. China.

b.Center of Materials Science and Optoelectronics Engineering, University of Chinese Academy of Sciences, Beijing 100049, P. R. China.

E-mail: zywen@mail.sic.ac.cn

c. University of Science and Technology of China, Hefei 230026, Anhui, China.

Experimental section

Material synthesis of the BM-LLZTO-CPE: A conventional solid state reaction (SSR) method is adopted to prepare cubic phase Ta-doped LLZO powder ($\text{Li}_{6.4}\text{La}_3\text{Zr}_{1.4}\text{Ta}_{0.6}\text{O}_{12}$ (LLZTO)), the detailed synthesis process was published in previous work^[1]. Then, the size of LLZTO was reduced to ~100 nm with the high-energy ball milling at a rotation speed of 400 rpm for 5 h on a Planetary Mill P-5 (Fritsch, Germany). LLZTO nanoparticles were dispersed in ethanol to produce 2 wt% suspension, and the excessive 1-methyl-3-trimethoxysilane imidazolium chloride (PMImCl, from Shanghai Cheng Jie Chemical Co. LTD.) was added to the suspension drop by drop at 70 °C with a mild stirring. After 12 h, the temperature was risen to 85 °C in order to volatilize the ethanol. Then, the grafted functionalized LLZTO (LLZTO-PMImCl) was washed with ethanol for several times and collected by centrifugation. At last, LLZTO-PMImCl and LiTFSI with a mol ratio of 1:1 was dissolved and reacted in deionized water in order to exchange the Cl^- with TFSI^- to obtain MB-LLZTO. The resulting substances were washed for 5-6 times with deionized water in order to remove residual Cl^- and then collected after centrifugation and dried at 80 for 24 h. Poly (ethylene oxide) (PEO, Mw 6×10^5 , 99%, form Acros), MB-LLZTO powders and lithium bis (trifluoromethanesulfonyl) imide ($\text{LiN}(\text{SO}_2\text{CF}_3)_2$, LiTFSI, 99%, from Sigma-Aldrich) were added in acetonitrile (CH_3CN , AR grade, 99.9%, Sigma) at a proportion of EO: Li=18:1 with 10 wt % solid content to form a homogeneous slurry under stirring for 8 h. The slurry was cast onto a PTFE plate. An electrolyte membrane (MB-LLZTO-CPE) was finally obtained after

vacuum dry 65 °C for 24 h. Composite polymer electrolyte with X% content of MB-LLZTO is denoted as X% MB-LLZTO.

Fabrication of battery

LiFePO₄ (from Tianjin STL Energy Technology Co., Ltd.) as the active material, equal Super P and VGCF as the conducting agents, and poly (vinylidene fluoride) (PVDF) as the binder were added in 1-methyl-2-pyrrolidinone (NMP) at the ratio of 8:1:1. The cathode slurry was mixed by planetary ball-milling machine at 250 rpm for 6 h. Then the slurry was cast to Al foil by a blade with 100 μm gap, and dried at 60 °C in vacuum oven for 24 h. The area mass of the acquired LiFePO₄ cathode is about 4 mg cm⁻². The S/C cathode was prepared by a common molten sulfur process, with the sulfur loading of about 1.0 mg cm⁻² and the details were published in our previous work^[2]. The all-solid-state lithium metal batteries were assembled with 12 mm lithium foil (from China Energy Lithium Co., Ltd.) as the anode, and the acquired electrolyte membrane (MB-LLZTO-CPE) as an electrolyte, then sealed them into the CR2320 coin cells by sealing machine (Shenzhen Kejing Star Technology Co., Ltd.).

Characterization

The morphology of samples was tested on a scanning electron microscope (SEM, SU-8200, Hitachi) and transmission electron microscope (TEM, JEM-2100F). The morphology of crystalline and amorphous phase was characterized by polarizing optical microscope (POM, Olympus BX53). X-ray diffraction (XRD) patterns of samples were tested on the Rigaku Ultima with Cu K α radiation from 10° to 80°. Differential scanning calorimetry (DSC) was performed on a PerkinElmer DSC 8000

ranging from -80 °C to 80 °C, with a heating rate of 10 °C min⁻¹. The thermogravimetric analysis (TGA, Netzsch 409PC) of samples were measured in Air atmosphere, with the heating rate of 10 °C min⁻¹. The granularity distribution of the ball-milling particles was tested by Malvern Mastersizer 3000.

⁶Li and ⁷Li MAS NMR experiments were carried out at 25 °C on a Bruker Advance III 400MHz Solid NMR Spectrometer, with a commercial 3.2 mm DVT probe. The ⁶Li spectra were acquired at Larmor frequency of 74.5 MHz with a recycle delay time of 10 s. The ⁷Li NMR experiment was performed at 193.1 MHz, with a delay time of 1 s. And the samples were spun at 15 kHz for direct polarization (DP). ^{6,7}Li NMR chemical shifts were referenced to LiCl solid powders (0 ppm). And the MestReNova was used to simulate the spectral resonances and to fit the peaks for analysis.

The ionic conductivities (σ) of electrolyte at different temperatures were acquired by electrochemical impedance spectroscopy (EIS) measurement using Autolab Metrohn 85167 system with frequency ranging from 0.1 Hz to 10⁶ Hz. The electrolyte membranes were sandwiched by two stainless steel plates (diameter of SS is 15.5mm) and sealed into CR2032 coin cells.

The value of lithium ionic conductivity was calculated by following equation:

$$\sigma = \frac{L}{S R}$$

where L represents the thickness of ceramic or electrolyte membrane, S is the contact area between electrolyte and electrode and R represents the bulk electrolyte resistance acquired from the EIS spectra.

The linear sweep voltammograms (LSV) measurement was carried out ranging from 2.5 to 6.5 V at 5 mV s⁻¹ scanning rate for Li/electrolyte/SS cell. The galvanostatic charge-discharge profiles and long cycle performance of battery were tested on a battery test system (LANHE CT2001A, Wuhan Land Electronic Co.Ltd.). The Li-LiFePO₄ and Li-S batteries were assembled in glove box (O₂<1ppm, H₂O<1ppm) using CR2025 coin cells, and the potential range in the charge-discharge process are 2.5-4.0 V and 1.0-3.0 V, respectively.

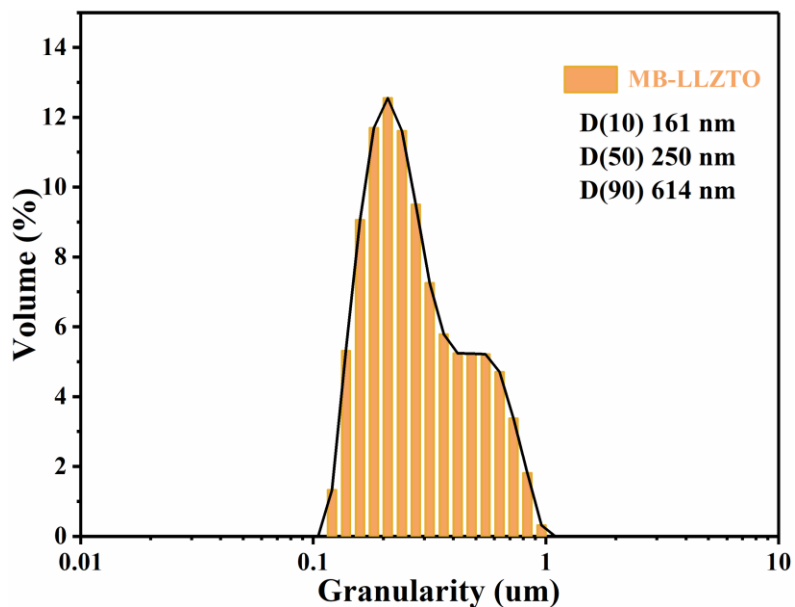


Figure S1. Distribution of particle sizes in the slurry of LLZTO after high-energy ball-milling.

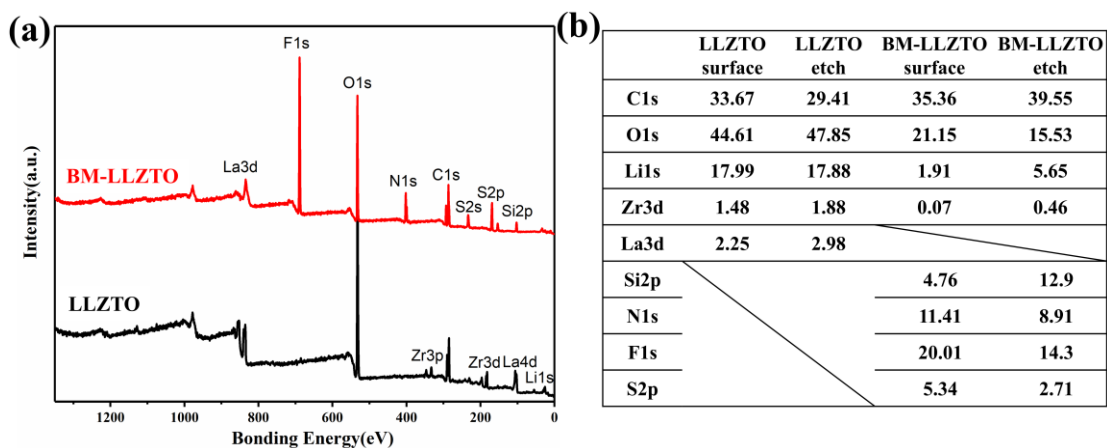


Figure S2. (a) The overall surface XPS spectra of the MB-LLZTO. (b) Comparisons of elements content before and after the molecular brushes grafting on the surface.

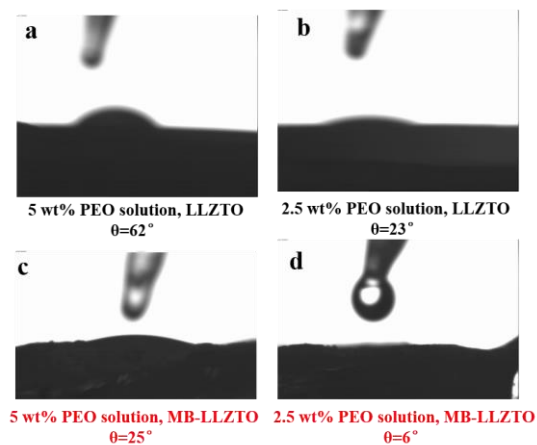


Figure S3. The contact angle between different content PEO solution (dissolved in acetonitrile) and (a) (b) pristine LLZTO sheet and (c) (d) MB-LLZTO tablet.

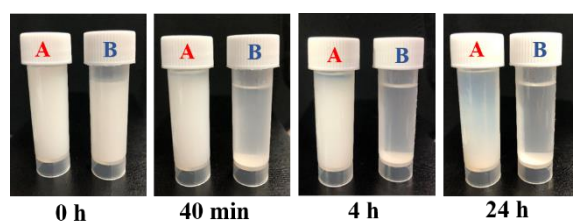


Figure S4. The optical photos comparisons of the acetonitrile suspension containing (A) pristine LLZTO and (B) MB-LLZTO nanoparticles over the standing time (40 min, 4 h, 24 h).

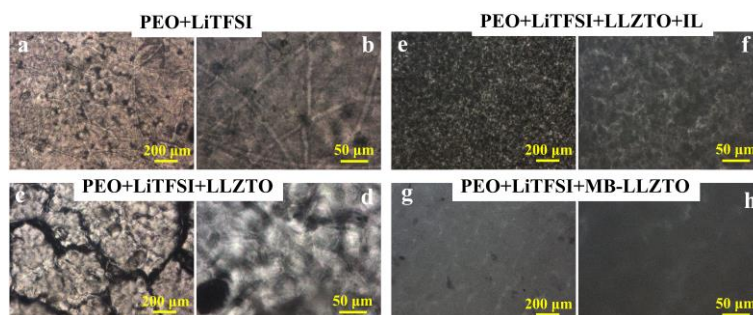


Figure S5. Polarization optical microscopy (POM) of composite polymer electrolyte with different additives.

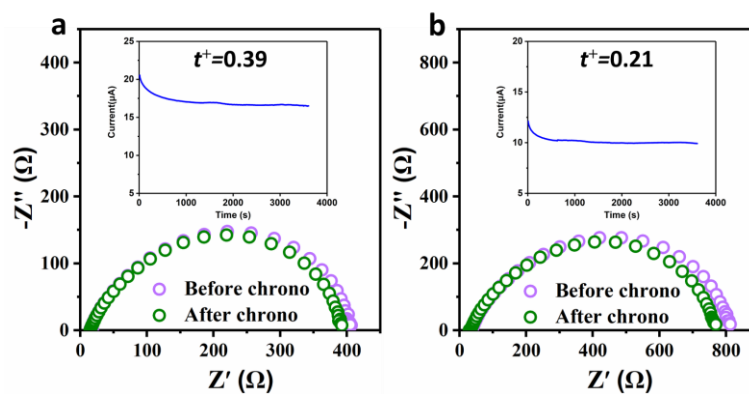


Figure S6. (a) (b) AC impedance spectra of the cells before and after the polarization. of the symmetric lithium metal cells based on 15% MB-LLZTO-CPE and control 0% CPE. Insert: Chronoamperometry curve at 10 mV and a duration time of 3600 s.

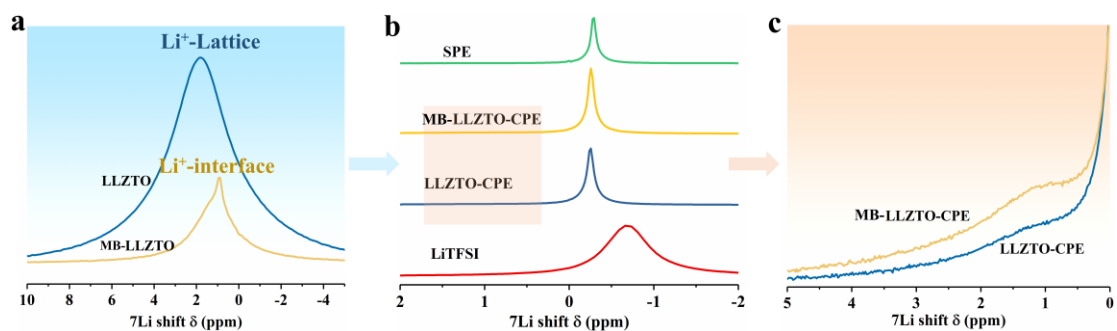


Figure S7. (a) ^7Li NMR of LLZTO and MB-LLZTO materials. (b) ^7Li direct polarization NMR spectra of local Li environments in LiTFSI, SPE, MB-LLZTO-CPE and LLZTO-CPE. (c) Magnification of assignments results for the LLZTO-CPE and MB-LLZTO-CPE.

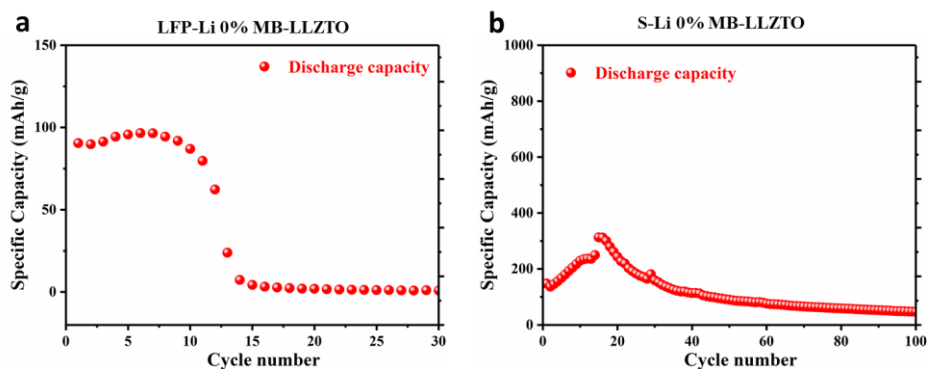


Figure S8. Cycling performance of LFP-Li and Li-S batteries based on 0% MB-LLZTO.

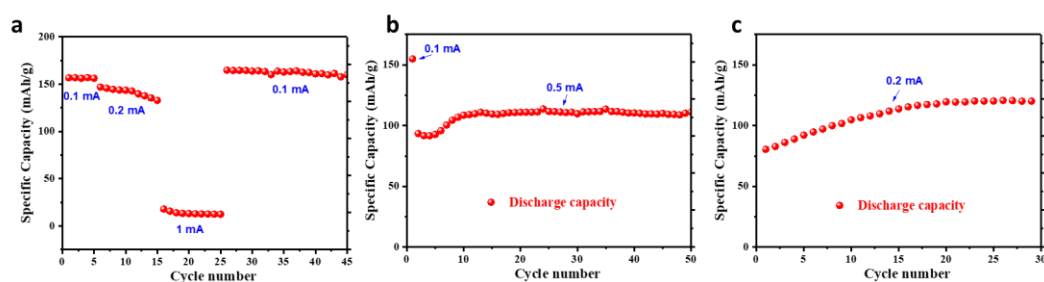


Figure S9. Rate performance and cycling performance of LFP/Li cells based on MB-LLZTO-CPE at variant current (0.5 mA and 0.2 mA).

Table S1. Comparison of the cycling performance for all-solid-state Li-S batteries reported from recent literatures.

Electrolyte	Sulfur cathode	Discharge capacity (mAh g ⁻¹), cycle (°C)	reference
PEO/LiTFSI+SiO ₂	S/mesoporous carbon	800, 25 cycles @70	[3]
PEO/LiTFSI+SSZ-13	S/Kejten black/Super P	980, 42 cycles @60	[2]
PEO/LiTFSI+MIL-53(Al)	S/macrostructural carbon	792, 50 cycles @80	[4]
PEO/LiTFSI+MMT	S@PAN@Mg _{0.6} Ni _{0.4} O/AB	634, 100 cycles @60	[5]
PEO/LiTFSI+LiN ₃	S/Kejten black	800, 30 cycles @70	[6]
PEO/LiTFSI+LLZTO	S/ Super P	360, 50 cycles @45	[7]
PEO/LiTFSI+ZrO ₂	N-CNs/S	986, 40 cycles @50	[8]
PEO/Garnet textile	Garnet textile-S	970, 40 cycles @60	[9]
PEO/LiTFSI+MB-LLZTO	S/Kejten black/Super P	750, 220 cycles @45	This

References:

- [1] X. Huang, T. Xiu, M. E. Badding, Z. Wen, *Ceramics International* **2018**, 44, 5660.
- [2] W. Li, S. Zhang, B. Wang, S. Gu, D. Xu, J. Wang, C. Chen, Z. Wen, *ACS Appl.*

- Mater. Interfaces* **2018**, 10, 23874.
- [3] X. Liang, Z. Wen, Y. Liu, H. Zhang, L. Huang, J. J. J. o. P. S. Jin, *J. Power Sources* **2011**, 196, 3655.
- [4] Y. Zhu, J. Li, J. J. J. o. P. S. Liu, *J. Power Sources* **2017**, 351, 17.
- [5] Y. Zhang, Y. Zhao, D. Gosselink, P. J. I. Chen, *Ionics* **2015**, 21, 381.
- [6] G. G. Eshetu, X. Judez, C. Li, O. Bondarchuk, L. M. Rodriguez-Martinez, H. Zhang, M. J. A. C. I. E. Armand, *Angew. Chem.-Int. Edit.* **2017**, 56, 15368.
- [7] Y.-X. Song, Y. Shi, J. Wan, S.-Y. Lang, X.-C. Hu, H.-J. Yan, B. Liu, Y.-G. Guo, R. Wen, L.-J. Wan, *Energy Environ. Sci.* **2019**, DOI: 10.1039/c9ee00578a.
- [8] O. Sheng, C. Jin, J. Luo, H. Yuan, C. Fang, H. Huang, Y. Gan, J. Zhang, Y. Xia, C. Liang, W. Zhang, X. Tao, *J. Mater. Chem. A* **2017**, 5, 12934.
- [9] Y. Gong, K. Fu, S. Xu, J. Dai, T. R. Hamann, L. Zhang, G. T. Hitz, Z. Fu, Z. Ma, D. W. McOwen, X. Han, L. Hu, E. D. Wachsman, *Materials Today* **2018**, 21, 594.